An Inexpensive Method for Measurements of Static Pressure Fluctuations

DAN LIBERZON AND LEV SHEMER

School of Mechanical Engineering, Tel Aviv University, Tel Aviv, Israel

(Manuscript received 24 June 2009, in final form 29 November 2009)

ABSTRACT

An application of a commercially available and inexpensive pressure probe and transducer, originally designed for pressure drop measurements in air conditioning conduits, is suggested for accurate and reliable measurements of static pressure fluctuations in airflow, with a particular application to wind interaction with water waves. It is demonstrated that this static pressure probe is a robust instrument that offers efficient dynamic pressure elimination while having low directional sensitivity and sufficiently high dynamic response. A series of measurements in a wind-wave flume was carried out to validate the characteristics of the sensor and of the pressure transducer.

1. Introduction

Static pressure fluctuations play an important role in momentum balance in turbulent boundary layer flows. In particular, fluctuations of static pressure in airflow over the water surface may contribute significantly to generation of water waves by wind (Jeffreys 1925; Phillips 1957). However, measurements of the static pressure fluctuations within the turbulent airflow boundary layer above water waves are not trivial, because they require decoupling of static pressure fluctuations from the (generally significantly stronger) fluctuations of dynamic pressure within the boundary layer; measurements of static pressure fluctuations can therefore be affected by variations in both the magnitude and the direction of the airflow. Accurate and reliable measurements of static pressure fluctuations thus require a probe that is insensitive to the mean and fluctuating dynamic pressure and to variations in the mean flow direction. In field experiments aimed at investigation of the airflow above lakes or sea, the boundary layer thickness is relatively large, so the spatial dimensions of the probe are less important. Quantitative data on wind–wave interaction, however, are often collected in laboratory facilities that offer an advantage of controllable experimental conditions. The boundary layer thickness in airflow over waves in a wind-wave tank is much narrower than that in the field experiments; thus, the probe required for such experiments should be as small as possible.

The lack of a convenient readily available instrument for accurate measurements of static pressure fluctuations in air above the wavy water surface has significantly hampered accumulation of extensive and reliable experimental data on wind–wave momentum exchange. Over the past decades, a number of static pressure measurement techniques, all using in-house made devices, were suggested. The common feature of various designs is a two-orifices sensing concept; the air flows around a flat symmetrical relative to the mean flow direction surface, with two or more sensing ports located on the opposing sides of that surface mutually eliminating the contribution of the dynamic pressure and thus sensitive to the static pressure fluctuations only. One of the most popular designs that can be manufactured relatively easy is the ‘‘disk’’ probe, which has been used in different modifications and sizes. In this probe the airflow is guided around a flat disk aligned with the mean flow, with the sensing ports located at both sides at the disk's center. First records of the use of such probes can be traced half a century back (Bryer et al. 1958). Further developments of this concept include the ‘‘two disks'' designs (Robertson 1972; Gill 1976), later improved by a ‘‘quad disk'' configuration (Nishiyama and Bedard 1991). These instruments proved to be successful in eliminating the effect of the dynamic pressure and offer a relatively low sensitivity to the variations in the angle of attack of the flow relative to the disks plane. Disk-type static pressure probes were successfully utilized for wind–wave interaction

Corresponding author address: Dan Liberzon, School of Mechanical Engineering, Tel Aviv University, Tel Aviv 69978, Israel. E-mail: liberzon@eng.tau.ac.il

DOI: 10.1175/2009JTECHA1352.1

studies (Papadimitrakis et al. 1986; Mastenbroek et al. 1996; Hare et al. 1997; Wilczak and Bedard 2004). At higher wind velocities, the disk-type pressure probes require larger disk diameter for efficient dynamic pressure elimination, thus making them less suitable for use in laboratory-scale wind-wave flumes.

A different version of the disk probe designed for laboratory use was proposed by Elliott (1972). The Elliott probe features streamlined upper and lower surfaces, introducing improved dynamic pressure elimination while preserving small probe diameter. The surface profile can be adjusted for the designed wind speed and attacking angles in each experiment empirically. The Elliott probe was used successfully in numerous studies by Donelan et al. (1999, 2005, 2006). This probe has to be designed and custom made for a particular experiment and requires precise manufacturing; its production is therefore time consuming and expensive.

Some alternative designs such as a cone-shaped probe (Snyder 1974; Snyder et al. 1981), as well as a spherical probe (Kataoka et al. 1989), can only be used in field experiments because of their relatively large size.

In this note, we examine application of a commercially available and inexpensive pressure probe and transducer, marketed mainly for applications in air conditioning systems, for accurate and reliable measurements of static pressure fluctuations in airflow over water waves. Experiments are carried out in a small-scale wind-wave flume. We demonstrate that the robust structure of the probe allows efficient dynamic pressure elimination while maintaining low directional sensitivity and sufficiently high dynamic response.

2. Experimental facility and method of validation

Experiments were performed in a facility designed for investigation of water-wave generation by wind that includes a closed-loop wind tunnel over a wave tank. The 5-m-long test section is made of clear glass and has a 0.4 m wide by 0.53 m high rectangular cross section. The water depth inside the test section is 0.2 m. Airflow is generated by a 5.5-kW personal computer (PC)-controlled blower. Closed-loop air circulation allows maintaining constant temperature and humidity during the experiments. Two large settling chambers, each having a volume of about 1 m^3, are located at the inlet and outlet of the test section. From the inlet settling chamber at which the airflow comes virtually to rest, the air is guided through a honeycomb and a contraction with the area ratio of 2.5:1 to the exit cross section of 0.28 m by 0.4 m with a close to uniform air velocity profile. To prevent airflow separation at the transition from the contraction exit plane to the 0.33 m by 0.4 m airflow part of the test section, a specially designed flap is installed. The system is capable of generating airflow with the mean velocity in the test section up to 20 m s^{-1}; however, to eliminate excessive noise, in the present experiments the air velocity did not exceed about 12 m s^{-1}. The energy of wind-generated waves is dissipated at the sloping beach made of porous material installed at the far end of the test section. To maintain constant airflow rate along the test section and to allow easy insertion of the sensors, a multisection Plexiglas roof is installed. The surface elevation is measured by using a pair of capacitance-type wave gauges, whereas the mean air velocity at any location within the cross section is measured by a single-ended 1-mm inner diameter Pitot tube. All sensors are mounted on an instrument carriage that can be moved along the test section. PC-controlled motorized linear traverse mechanisms on the carriage allow precise positioning of the probes. Additional details about the wind-wave facility and instrumentation can be found at the Tel Aviv University (TAU) Laboratory Web site (available online at http://www.eng.tau.ac.il/research/laboratories/waves/wind_wave_flume.html).

To enable accurate static pressure variations measurements close to the water surface, low directional sensitivity and sufficiently high frequency response of the instrument are essential. The present study examines the suitability for those purposes of a commercially available static pressure probe A520 coupled with a differential pressure transducer (PR274), both manufactured by MAMAC Systems, Inc. (available online at http://www.mamacsys.com/).

The probe consists of a 0.2-m-long aluminum tube 8 mm in diameter, equipped with two opposing orifices 2 mm in diameter, located 12 mm from the end of the probe. The sensing part of the probe is enclosed by a 25-mm-long plastic case with the outer diameter of 10 mm. The plastic case seals the front end of the probe and has a narrow gap at its far end; the probe thus is sensitive to the static pressure at the distance of 25 mm from its end. The pressure difference between the probe location and the atmospheric pressure outside of the test section is measured by recording the instantaneous output voltage of the pressure transducer with sensitivity of 0.000 25 Pa. Both the probe and the atmospheric sensing ports are connected to the pressure transducer by a 6-mm inner diameter, 30-cm-long Tygon tubes. To eliminate fluctuations, the tube end at the atmospheric pressure sensing side is enclosed inside a 3 cm^3 rigid box filled with sponge. Special care was taken to switch off the air conditioning in the laboratory during the measurements.

The sensitivity of the probe to the dynamic pressure variations was investigated first. To this end, the static pressure along the test section was measured and the pressure drop was compared with estimates based on

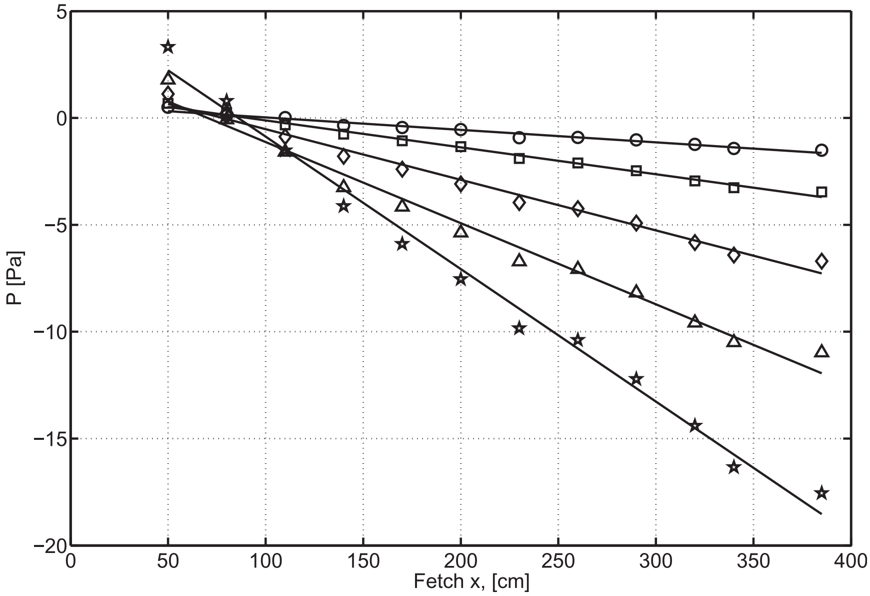

FIG. 1. Pressure variation along the test section for various maximum air velocities U_{max}: 2.78 (circles), 4.36 (squares), 5.94 (diamonds), 7.49 (triangles), and 8.93 m s^{-1} (stars).

pipe flow analogy. Mean wind velocity was determined by measuring the wind velocity at the contraction exit cross section at which the velocity is uniform, taking into account the cross-sectional area ratio. The estimated pressure drop in the test section was calculated using the hydraulic diameter of the test section $D = 0.362$ m and assuming smooth walls. Measurements were performed for a number of mean wind velocities. At each location, the pressure was measured at the height of 0.11 m above the wavy water surface at a sampling frequency of 120 Hz for the duration of 60 s (Fig. 1).

Because of the pressure buildup at the test section entrance, the measured values close to the entrance are somewhat higher than the atmospheric pressure. Nevertheless, the significant changes (of the order of magnitude) in the dynamic pressure for different flow velocities have practically no effect on the measured static pressure. For every flow rate studied, the pressure varies essentially linearly along the flume. The total measured pressure variation along the test section is less than 3 Pa for $U_{mean} = 2.78$ m s^{-1} and increases to about 20 Pa for $U_{mean} = 8.93$ m s^{-1}. For low wind velocities, the mean static pressures measured at consecutive stations differ by a small fraction of 1 Pa, thus demonstrating the high accuracy of the sensor. The measured pressure gradient is of the same order as the computed for a smooth pipe flow with an identical hydraulic diameter. The measured values are about 2.5 times higher than the calculated values for the smooth pipe pressure gradient ($\partial p/\partial x = 0.61$ Pa m^{-1} measured as compared to $\partial p/\partial x = 0.26$ Pa m^{-1} calculated for $U_{mean} = 2.78$ m s^{-1}; for a higher mean velocity of $U_{mean} = 8.93$ m s^{-1}, the corresponding values are $\partial p/\partial x = 5.32$ Pa m^{-1} and $\partial p/\partial x = 1.98$ Pa m^{-1}). The higher pressure gradient values in the flume as compared to smooth pipe are expected because of the roughness of the wavy water surface and momentum transfer from air to water flow.

To examine the directional sensitivity of the instrument, the probe was mounted on a rotating holder and measurements were carried out at different angles of the probe axis alignment relative to the mean flow direction (see Fig. 2). The probe in these measurements was positioned within the wind tunnel exit section above the horizontal part of the flap, where the airflow is unidirectional and unaffected by waves.

In Fig. 2 the results show a quite weak dependence of the measured static pressure on the probe axis angle and on the mean flow velocity. Even for a relatively large flow rate corresponding to $U_{mean} = 8.93$ m s^{-1}, the error in the static pressure due to misalignment of the probe axis with the flow direction does not exceed 1.5 Pa, as long as the misalignment angle remains within about 7°. The angular sensitivity of the probe is thus comparable to that of the Elliott probe. The actual probe axis–wind direction misalignment in wind-wave generation experiments can be estimated from the ratio of the maximum possible vertical velocity component $v = a_0\omega_0$, where a_0 and ω_0 are the dominant wave amplitude and radian frequency, respectively, and the air velocity U is at the lowest measuring location. Because the probe size prevents

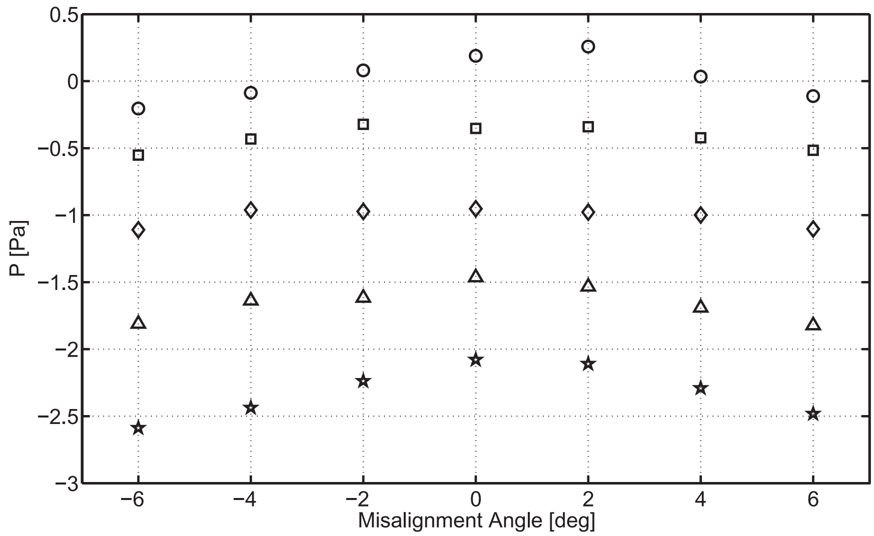

FIG. 2. The dependence of the measured static pressure on the probe axis direction relative to the mean flow. Symbols as in Fig. 1.

measurements lower than about 5 mm above the highest possible wave at any given condition, this ratio yields misalignment angles that mostly do not exceed about 5°. Although turbulent fluctuations can cause some additional increase in the misalignment error, the measured low angular sensitivity of the probe ensures high accuracy of pressure fluctuation measurements, even close to the water surface.

To evaluate further the contribution of the error in static pressure resulting from probe axis misalignment with the instantaneous wind direction to the accuracy of measurements of momentum transfer between wind and waves due to fluctuations in the static pressure, the following considerations have to be taken into account: The momentum transfer depends on the amplitude and the phase of the static pressure fluctuations due to the presence of the waves that are approximately 180° out of phase with the surface elevation. On the other hand, the vertical velocity component at the air–water interface is shifted by 90° relative to the surface elevation. The misalignment angle fluctuations are roughly in phase with the vertical velocity component and are shifted therefore by about 90° relative to the static pressure fluctuations. Hence, the misalignment angles are large mostly when the instantaneous static pressure fluctuations are low and vise versa. The phase relations ensure that the misalignment error has a vanishing effect on the amplitude and phase of the measured pressure fluctuations. These considerations, as well as the results of Figs. 1 and 2, thus demonstrate that, for the expected range of the forcing wind velocities and air velocity direction variations, the pressure sensor is essentially insensitive to both the dynamic pressure and misalignment angle variations.

The probe's dynamic response is an additional essential feature that requires examination. The airflow over water waves is affected by surface elevation variations in space and time, causing corresponding variations in the static pressure. As mentioned above, reliable monitoring of the phase (relative to the surface elevation) of the pressure fluctuations in the air boundary layer at each frequency present in the wave spectrum is indispensable for understanding the energy and momentum transfer mechanism during water-wave excitation by wind. Even in a small experimental facility, the frequencies of water waves do not exceed about 10 Hz; thus, the phase response of the static pressure measurement system was examined for frequencies ranging from 1 to 10 Hz. To this end, a 6-ft speaker was mounted at the sidewall of a wooden acoustic box (0.5 m × 0.5 m × 0.5 m), and the speaker membrane fluctuations were driven by a monochromatic driving voltage from a signal generator at various frequencies, thus creating static pressure fluctuations within the box. Instantaneous displacements of the membrane were measured by an optic displacement sensor mounted on the outer side of the membrane. The static pressure probe was introduced to the box through a small opening in the wall and connected to the transducer by a Tygon tube similar in length to the one used in the wind-wave flume. The probe's directional sensitivity was tested first. These tests show that the measured pressure fluctuations are not affected by the sensor rotation around its axis, as well as by positioning the probe at different locations within the box and at different angles relative to the speaker's plane.

It is well known (Elliott 1972; Papadimitrakis et al. 1986) that pressure sensors introduce phase lag that has to

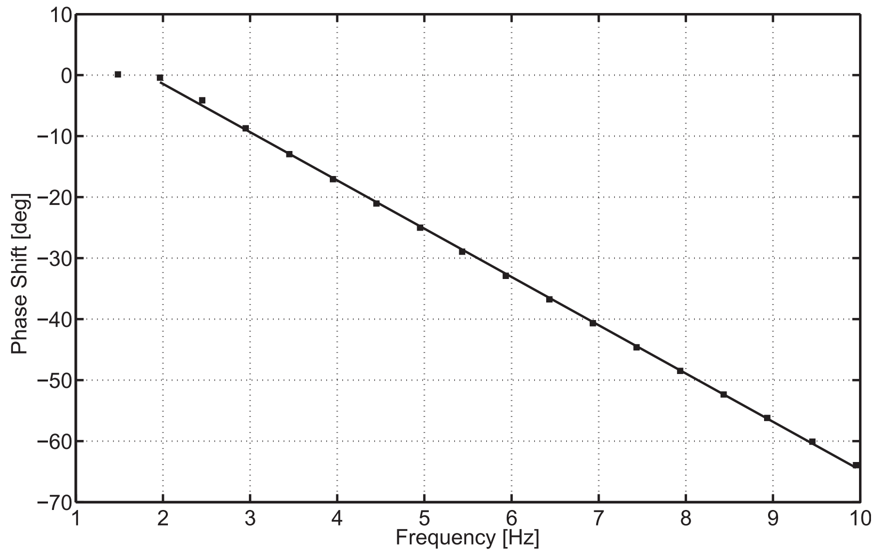

FIG. 3. The phase shift introduced by the instrument of the pressure fluctuations as a function of frequency. Squares represent measured phase lag, and the solid line represents linear fit.

be taken into account when momentum and energy flux balances are evaluated at air–water interface. To determine the actual phase lag resulting from the instrument response, both the transducer and the optic displacement sensor output signals were recorded simultaneously; in each case, the duration of continuous record was 60 s. The recorded phase shifts relative to the optic displacement sensor at various speaker driving frequencies are plotted in Fig. 3. The measured pressure phase lag values increase linearly with frequency, exhibiting behavior similar to that observed for the static pressure sensors used by, for example, Elliott (1972) and Papadimitrakis et al. (1986).

For an accurate estimation of wind–wave momentum exchange rates, the pressure fluctuations at the wavy interface have to be known. However, pressure fluctuations vary significantly with the distance from the water surface, whereas the size of the sensor prevents measurements in the immediate vicinity of the air–water interface. To enable estimation of the pressure fluctuation amplitude at the mean water surface level, the vertical probe location relative to the mean water surface has to be known. To this end, a special resistance-type water-surface sensor was built. The sensor placed in air above the water consisted of two vertical wires with exposed tips spaced by about 2 mm; the sensor can be moved vertically by a computer-controlled stepping motor with accuracy better than 0.1 mm. Because of the large difference in the electrical conductivity between water and air, the output signal indicated the presence of either liquid or air at the probe tip at each instant. The lowest sensor position at which the probe tip remained dry throughout the whole prescribed recording duration allowed the determination of the maximum possible surface elevation for the given operational conditions and the probe location along the test section. The value of the maximum surface elevation relative to the mean water surface could be determined from the wave gauge records. The pressure probe was located above the tip of the interface sensor with a known vertical spacing. This arrangement thus made it possible to determine the vertical location of the pressure probe relative to the mean air–water interface. The instantaneous static pressure variation with time, measured at the height of 15 mm above the wavy water surface at mean cross-sectional velocity of 9.5 m s^{-1}, was juxtaposed with the surface elevation signal simultaneously recorded at the same location along the test section, $x = 3.95$ m. The pressure fluctuations in the air boundary layer close to the water surface are expected to contain harmonics that constitute the surface elevation spectrum; in the absence of energy transfer from wind to waves, a phase shift of 180° between surface elevation and pressure variations is expected (Papadimitrakis et al. 1986; Donelan et al. 2006). Simultaneous pressure and surface elevation records in Fig. 4 indeed demonstrate strong correlation between the two signals, with the pressure fluctuations at the dominant frequency shifted by about 180° relative to the wave gauge output, as expected in the absence of energy transfer from wind to waves (Papadimitrakis et al. 1986; Donelan et al. 2006).

To test the performance of the static pressure probe in the flume, simultaneous measurements of surface elevation and static pressure fluctuations were carried out at various heights above the water surface. Cross-spectral

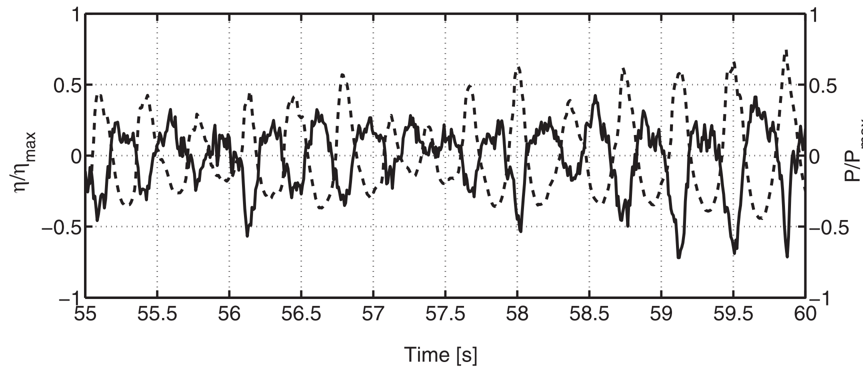

FIG. 4. A 1-min-long extract of the simultaneous records of the surface elevation and of the static pressure variation measured at the height of 15 mm above the highest possible wave. Both parameters are normalized by their respective highest measured (during the whole duration of the record) values ($\eta_{\max} = 20.2$ mm, $P_{\max} = 9.3$ Pa). The solid curve represents static pressure, and the dashed curve represents surface elevation.

analysis of the static pressure and the surface elevation fluctuations allows determining the magnitude squared coherence (MSC) as a function of frequency:

$$\mathrm{MSC}(f) = \frac{|P_{p\eta}(f)|^2}{P_{pp}(f)P_{\eta\eta}(f)},$$

where $P_{\eta\eta}$ and P_{pp} are the power spectra surface elevation and the static pressure, respectively, and $P_{P\eta}$ is the cross-spectrum (Therrien 1992). The values of MSC at four representative heights above the mean water level are presented in Fig. 5, and the corresponding pressure and surface elevation variations power spectra are presented in Figs. 6a,b. The coherence between the surface elevation and the static pressure fluctuations at all vertical locations of the pressure sensor in the vicinity of the dominant wave frequency of $f = 2.76$ Hz exceeds 0.8. Moreover, notable coherence between these two parameters exists also at twice the dominant frequency, thus indicating that, in the strongly nonlinear wind-wave field, the pressure fluctuations are strongly affected also by the second-order bound waves. However, the effect of the bound waves decays fast with the distance from the interface.

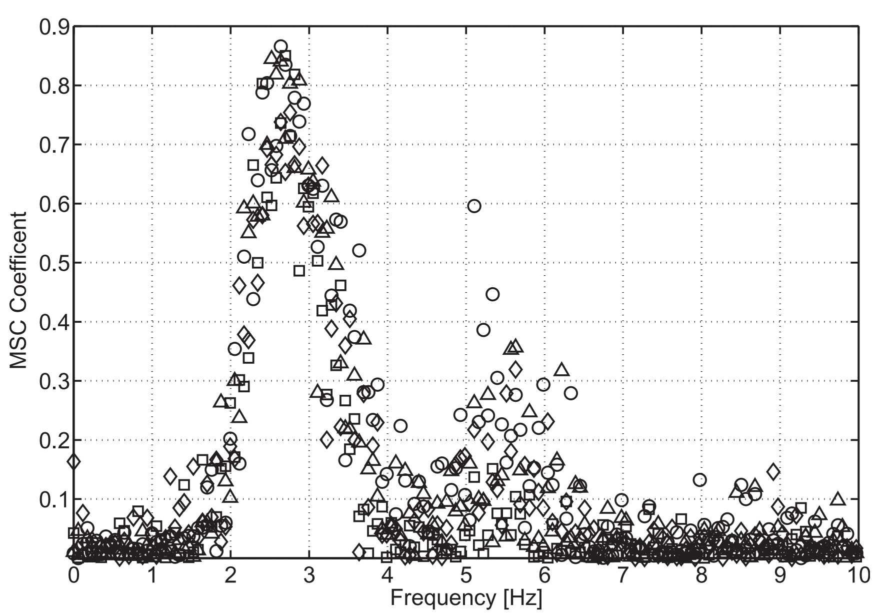

FIG. 5. Dependence of the MSC on frequency at various positions z above the mean water level: 26 (circles), 31 (triangles), 38 (diamonds), and 47 mm (squares).

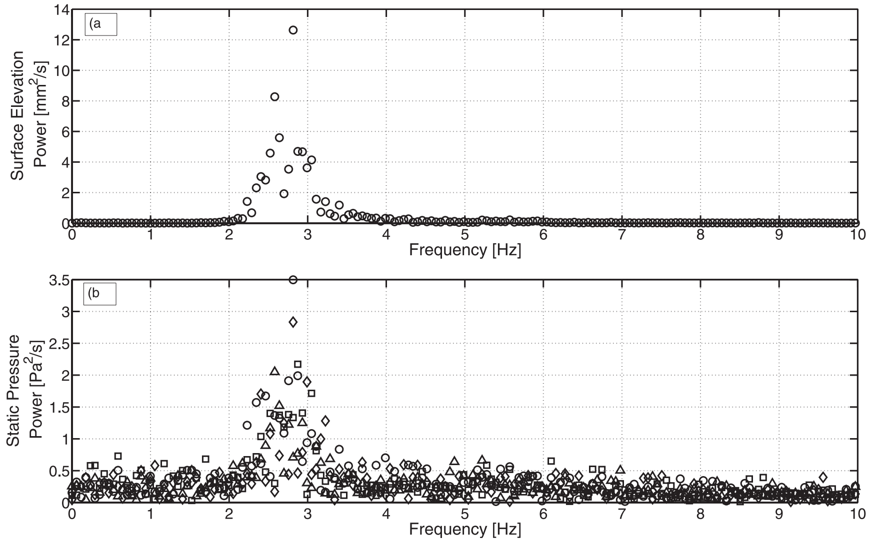

FIG. 6. The power spectra of (a) surface elevation fluctuations and (b) static pressure variations, with symbols as in Fig. 5.

The phase of the cross-spectrum $P_{P\eta}$ for those frequencies where the correlation between the surface elevation and the pressure fluctuations is significant (MSC > 0.6) was corrected according to the instrument phase response and is plotted in Fig. 7. The phase shift between the two signals seems to be independent of frequency and of the vertical location of the pressure probe, and it remains smaller than 180° by 10°–30°. These results are in agreement with the data of Donelan et al. (2006) and Hare et al. (1997), among others.

The amplitude of the static pressure fluctuations around the dominant frequency at each height above the mean water level z was calculated as

$$p_{\rm rms} = \left(\sum_{f_{\rm min}}^{f_{\rm max}} P_{pp}(f)\Delta f\right)^{1/2},$$

where $f_{\rm min}$ and $f_{\rm max}$ correspond to the lower and upper boundaries, respectively, of the frequency domain where MSC > 0.6. The variation of P with z is plotted in Fig. 8.

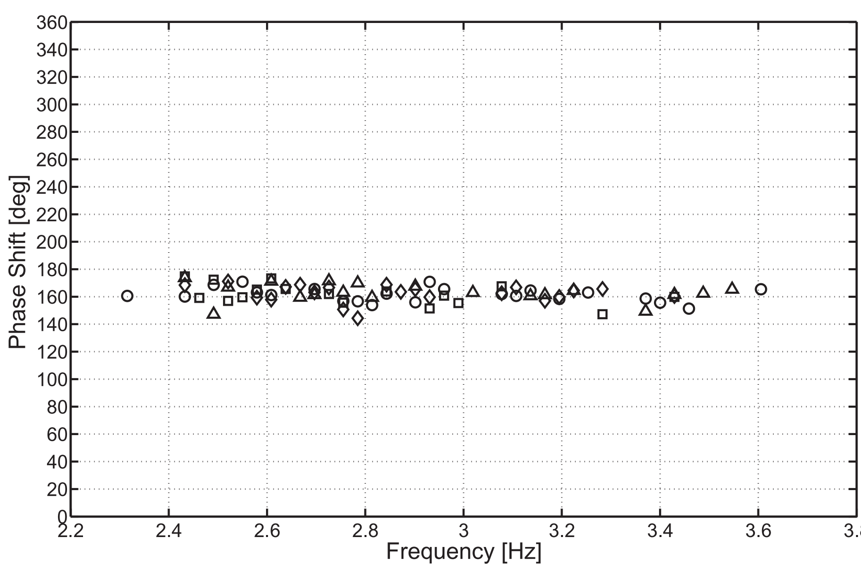

FIG. 7. The phase of the cross-spectrum $P_{P\eta}$ for frequencies where MSC exceeds 0.6, with symbols as in Fig. 5.

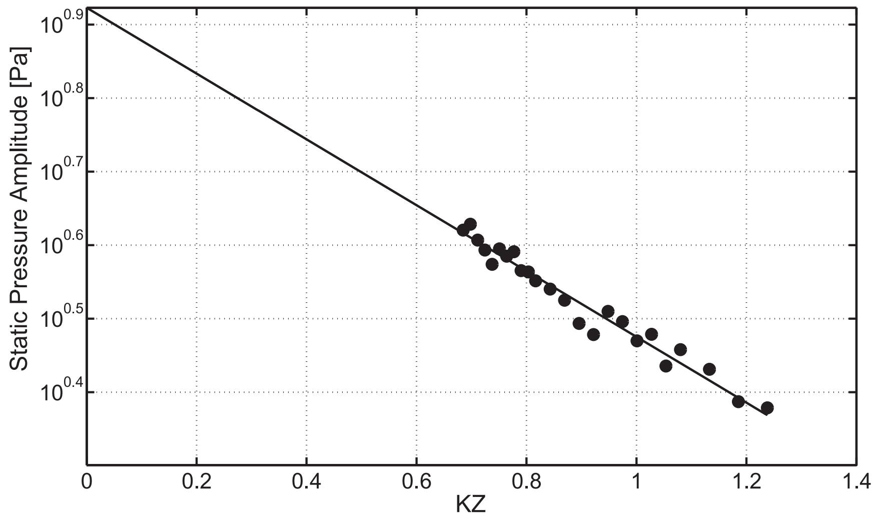

FIG. 8. Static pressure fluctuations amplitude as function of kz at $x = 3.95$ m, $U_{max} = 9.5$ m s^{-1}. The circles represent the data, and the solid line represents exponential fit $P(z) = P_0 \exp(-\alpha kz)$.

In view of strong coherence between the surface elevation and the static pressure fluctuations, it is reasonable to render the vertical coordinate dimensionless using the dominant water wavenumber $k = 2\pi/\lambda$. For the present experimental conditions, the dominant wavelength $\lambda = 0.21$ m, yielding $k = 29.91$ m^{-1}. In Fig. 8 the results show that the amplitude of the static pressure fluctuations decays exponentially with the height

$$P(z) = P_0 e^{-\alpha kz}.$$

The best fit yields the value of the coefficient $\alpha = 1.03$ so that the extrapolated value of the pressure fluctuations amplitude at the mean surface level $P_0 = 8.37$ Pa.

3. Conclusions

The possibility to use a readily available instrument originally designed for static pressure measurements in air conditioning systems, for accurate pressure measurements in the boundary layer in air above water waves, is demonstrated. In the course of the validation tests, the probe has shown excellent dynamic pressure elimination ability, more than adequate frequency response, and very weak directional sensitivity. The cross-spectral analysis clearly demonstrates the instrument's capability to measure static pressure fluctuations at frequencies typical for laboratory and field experiments on water-wave interaction with wind. The performance of the sensor is comparable with such instruments as the Elliott probe, which is used extensively in laboratory studies of wind waves. Moreover, relatively small dimensions of the probe allow spatial resolution that is better than that of most custom-made probes that have been employed for wind-wave generation studies. Because of the need to rely on expensive, specially designed probes in those experiments, only limited data exist on the pressure fluctuations above wind waves, in spite of the crucial role those fluctuations play in the air–water momentum balance. Application of a readily available instrument can contribute significantly to the progress in wind–wave interaction studies, both in laboratory studies and in field experiments over sea and lakes.

Acknowledgments. The authors acknowledge that the support of this study is supported by Grant 1194/07 from the Israeli Science Foundation.

REFERENCES

Bryer, D. W., D. E. Walshe, and H. C. Garner, 1958: Pressure probes selected for three-dimensional flow measurement. Aeronautical Research Council Rep. 3037, 28 pp.

Donelan, M. A., N. Madsen, K. K. Kahma, I. K. Tsanis, and W. M. Drennan, 1999: Apparatus for atmospheric surface layer measurements over waves. *J. Atmos. Oceanic Technol.,* **16,** 1172–1182.

——, A. V. Babanin, I. R. Young, M. L. Banner, and C. McCormick, 2005: Wave follower field measurements of the wind-input spectral function. Part I: Measurements and calibrations. *J. Atmos. Oceanic Technol.,* **22,** 799–813.

——, ——, ——, and ——, 2006: Wave-follower field measurements of the wind-input spectral function. Part II: Parameterization of the wind input. *J. Phys. Oceanogr.,* **36,** 1672–1689.

Elliott, J. A., 1972: Instrumentation for measuring static pressure fluctuations within the atmospheric boundary layer. *Bound.-Layer Meteor.,* **2,** 476–495.

Gill, G. C., 1976: Development and testing of a non-moving-parts static pressure inlet for use on ocean buoys. University of Michigan Rep., NOAA 01-6-038-115, 43 pp.

Hare, J. E., T. Hara, J. B. Edson, and J. M. Wilczak, 1997: A similarity analysis of the structure of airflow over surface waves. *J. Phys. Oceanogr.,* **27,** 1018–1037.

Jeffreys, H., 1925: On the formation of water waves by wind. *Proc. Roy. Soc. London,* **107A,** 189–206.

Kataoka, T., Y. Mitsuta, and O. Tsukamoto, 1989: The development of a fast response static pressure instrument for field use. *J. Meteor. Soc. Japan,* **67,** 351–357.

Mastenbroek, C., V. K. Makin, M. H. Garat, and J. P. Giovanangeli, 1996: Experimental evidence of the rapid distortion of turbulence in the air flow over water waves. *J. Fluid Mech.,* **318,** 273–302.

Nishiyama, R. T., and A. J. Bedard Jr., 1991: A ''Quad-Disc'' static pressure probe for measurement in adverse atmospheres: With a comparative review of static pressure probe designs. *Rev. Sci. Instrum.,* **62,** 2193–2204.

Papadimitrakis, Y. A., E. Y. Hsu, and R. L. Street, 1986: The role of wave-induced pressure fluctuations in the transfer processes across an air-water interface. *J. Fluid Mech.,* **170,** 113–137.

Phillips, O. M., 1957: On generation of waves by turbulent wind. *J. Fluid Mech.,* **2,** 417–495.

Robertson, P., 1972: A direction-insensitive static head sensor. *J. Phys.,* **5E,** 1080–1082.

Snyder, R. L., 1974: A field study of wave-induced pressure fluctuations above surface gravity waves. *J. Mar. Res.,* **32,** 497–531.

——, F. W. Dobson, J. A. Elliott, and R. B. Long, 1981: Array measurements of atmospheric pressure fluctuations above surface gravity waves. *J. Fluid Mech.,* **102,** 1–59.

Therrien, C. W., 1992: *Discrete Random Signals and Statistical Signal Processing.* Prentice Hall, 576 pp.

Wilczak, J. M., and A. J. Bedard, 2004: A new turbulence microbarometer and its evaluation using the budget of horizontal heat flux. *J. Atmos. Oceanic Technol.,* **21,** 1170–1181.